

# DETECTION OF CO(4–3), CO(9–8), AND DUST EMISSION IN THE BAL QUASAR APM 08279+5255 AT A REDSHIFT OF 3.9

D. Downes and R. Neri

Institut de Radio Astronomie Millimétrique, 38406 St. Martin d'Hères, France

T. Wiklind

Onsala Space Observatory, S-43992 Onsala, Sweden

D. J. Wilner

Harvard-Smithsonian Center for Astrophysics, Cambridge, MA 02138

and

P. A. Shaver

European Southern Observatory, D-85648 Garching bei München, Germany

## ABSTRACT

We detected with the IRAM interferometer the lines of CO(4–3) and CO(9–8) from the recently-discovered broad absorption line quasar APM 08279+5255. The molecular lines are at a redshift of 3.911, which we take to be the true cosmological redshift of the quasar's host galaxy. This means the quasar emission lines at  $z = 3.87$  are blueshifted by a kinematic component of  $-2500 \text{ km s}^{-1}$ , and, along with the broad absorption lines, are probably emitted in the quasar's wind or jet, moving toward us. The CO line ratios suggest the molecular gas is at a temperature of  $\sim 200 \text{ K}$ , at a density of  $\sim 4000 \text{ cm}^{-3}$ . We also detected the dust emission at 94 and 214 GHz (emitted wavelengths 650 and  $290 \mu\text{m}$ ). The spectral index of the mm/submm continuum is +3.2, indicating the dust emission is optically thin in this part of the spectrum. The extremely high CO and dust luminosities suggest magnification by gravitational lensing. Using the optical extent and our limit on the size of the CO region, we estimate a magnification of 7 to 30 for the CO lines and the far-IR continuum, and 14 to 60 for the optical/UV. In this interpretation, the molecular gas and dust is in a nuclear disk of radius 90 to 270 pc around the quasar. The quasar is 25 to 100 times stronger than, but otherwise resembles, the nucleus of Mrk 231.

*Subject headings:* galaxies: quasars — galaxies: individual: (APM 08279+5255) — galaxies: active — galaxies: ISM — cosmology: gravitational lensing — radio lines: galaxies

The recently-discovered broad absorption line (BAL) quasar APM 08279+5255 (Irwin et al. 1998) at  $z = 3.87$  has an astounding luminosity of  $5 \times 10^{15} L_{\odot}$ , making it the most luminous object in the Universe.<sup>1</sup> Ledoux et al. (1998) found that the source consists of two components separated by  $0.35''$  with similar spectra. Together with the extraordinary luminosity, this strongly suggests the source is gravitationally lensed, probably by one of the absorption-line systems along the line of sight (Irwin et al. 1998). The IRAS fluxes and the submillimeter detections with the SCUBA bolometers indicate the presence of warm dust, with an infrared component at a temperature of  $\sim 200$  K (Lewis et al. 1998). The source is obviously similar to the gravitationally lensed sources IRAS F10214+4724 at  $z = 2.3$  and the Cloverleaf quasar at  $z = 2.6$  (e.g., Serjeant et al. 1998; Kneib et al. 1998). In this Letter, we present observations of APM08279+5255 in the 1 and 3 mm continuum and in CO lines from warm, dense, molecular gas.

We observed this remarkable object with the IRAM Plateau de Bure interferometer and detected both the CO(4–3) and CO(9–8) lines at  $+2500 \text{ km s}^{-1}$  relative to  $z = 3.87$ . We also detected dust continuum emission, redshifted to 1.4 and 3.2 mm. The observations were done in August and November 1998 with the antennas on baselines from 24 to 160 m, giving synthesized beams of  $6.6'' \times 5.3''$  at 94 GHz and  $3.2'' \times 2.3''$  at 211 GHz. Receiver temperatures were 45 to 65 K at both frequencies. The spectral correlators covered  $1400 \text{ km s}^{-1}$  at 3.2 mm and  $760 \text{ km s}^{-1}$  at 1.4 mm, with resolutions of 8 and  $4 \text{ km s}^{-1}$  respectively. Amplitudes were calibrated with the strong sources 3C454.3, 3C273, 0923+392, and MWC 349, and phases were calibrated with 4C54.15 and 0804+499. **Table 1** summarizes our results.

We interpret the redshift,  $z = 3.911$ , of the CO(4–3) and CO(9–8) lines as being the true cosmological redshift of the quasar’s host object. The optical redshift of  $z = 3.87$ , derived from high excitation lines (Irwin et al. 1998), thus corresponds to gas flowing toward us, with a kinematic blueshift of  $2500 \text{ km s}^{-1}$  relative to the molecular gas. Quasar high-excitation lines are usually blueshifted by 500 to  $1000 \text{ km s}^{-1}$  relative to low excitation lines (e.g., Storrie-Lombardi et al. 1996). In addition to the main optical emission lines, Ledoux et al. (1998) found an NV doublet in absorption at  $z = 3.901$  and Irwin (1998) found several CIV doublets up to  $z = 3.92$ , so there is also some highly ionized gas at velocities close to the CO redshift. The CO(4–3) line from APM 08279+5255 has a line width of  $480 \text{ km s}^{-1}$  (FWHM) (Fig. 1), typical of line widths from rotating nuclear disks of molecular gas in ultraluminous IR galaxies (e.g. Downes & Solomon 1998).

The images in Fig. 1 show a source that coincides within  $0''.3$  of the optical quasar

---

<sup>1</sup>We use  $H_0 = 50 \text{ km s}^{-1} \text{ Mpc}^{-1}$  and  $q_0 = 0.5$  throughout this paper.

(revised optical position from Irwin 1998), and with the non-thermal radio source detected at 1.4 GHz (White et al. 1997). The interferometer beams are thus far too large to show source sizes or velocity gradients. Higher-resolution observations are now in course. A tentative size of the CO emission region has been obtained from  $u, v$  plane fits to the CO(9–8) data. Although noisy, it implies a CO source size of  $0''.8 \pm 0''.2$ .

The continuum fluxes were derived from the line-free channels at 3.2 mm, and from the upper sideband measurements at 1.4 mm to avoid contamination from the CO lines. The corresponding emitted wavelengths are 290 and  $650 \mu\text{m}$ , i.e., dust radiation in the far-IR/sub mm range. The fluxes are given in Table 1. In this part of the spectrum, the continuum spectral index is +3.2, corresponding to optically thin dust. Our 1.4 mm flux of 17 mJy is somewhat lower than that quoted by Lewis et al. (1998) from wideband bolometer measurements, but probably consistent within the errors.

Although we lack a more precise size measurement for the time being, we can deduce a number of constraints on the source from the CO and dust detections.

1) *The gas is hot.* The CO  $J = 9$  level is  $J(J + 1) \times 2.77 \text{ K} = 249 \text{ K}$  above the ground state, and in normal galactic spiral-arm molecular clouds, the typical  $\text{H}_2$  densities of  $\sim 300 \text{ cm}^{-3}$  are not sufficient to collisionally populate the CO  $J = 9$  level. Therefore the mere detection of the CO(9–8) line shows the gas is hot and dense. Could the gas be radiatively excited by the quasar? Maloney, Begelman, & Rees (1994) showed that dense gas can survive in molecular form close to an AGN. The strong radial dependence of radiative excitation in their model, however, plus the large dust mass, the large dust opacity at short wavelengths, and the inferred extent of the molecular gas distribution (see below), make it unlikely that the quasar’s radiation can affect a significant volume of gas. We therefore think the CO is collisionally excited.

Lewis et al. (1998) fit a blackbody curve to the sub-mm continuum and obtained a dust temperature of 220 K. One can also fit a two-temperature model, with a cool, optically thin, far-IR component and a hot, opaque, mid-IR component. However, even with this fit, the “cool” component must be at  $> 150 \text{ K}$ . Our escape-probability radiative transfer models show that if the gas temperature is 140 to 250 K, with an  $\text{H}_2$  density of  $\sim 4000 \text{ cm}^{-3}$ , in a cosmic blackbody background field of  $(1 + z) \times 2.7 \text{ K}$ , then collisional excitation yields CO level populations that cause the line brightness temperature of CO(9–8) to be about half that of CO(4–3). Hence the integrated flux, in  $\text{Jy km s}^{-1}$ , of CO(9–8) should be about 2.5 times that of CO(4–3), as is observed.

2) *If the CO source size is  $0''.6$  to  $1''.0$ , as indicated by our data thus far, then the gravitational lens must magnify the CO lines by a factor of 7 to 20.* The reasoning is as

follows. The apparent CO luminosity is

$$L'_{\text{CO}}(\text{obs}) = 363 (S\Delta V) \lambda^2 D_A^2 (1+z) \quad , \quad (1)$$

where  $(S\Delta V)$  is the integrated line flux in  $\text{Jy km s}^{-1}$ ,  $\lambda$  is the observed wavelength in mm, and  $D_A$  is the emission distance (= angular size distance) in Mpc (this may be derived from eq.(1) of Solomon, Downes, & Radford (1992)). The lens magnification of the CO can then be estimated from eq.(2) of Downes, Solomon, & Radford (1995) to be

$$m_{\text{CO}} = \frac{a}{R} = \frac{\pi a^2 \Delta V}{L'_{\text{CO}}(\text{obs})} f_V T_b \quad . \quad (2)$$

where  $a$  is the apparent semi-major axis of the magnified CO source, in pc,  $\Delta V$  is the line width in  $\text{km s}^{-1}$ ,  $L'_{\text{CO}}$  is the apparent (magnified) CO luminosity in  $\text{K km s}^{-1} \text{pc}^2$ ,  $R$  is the true source radius in pc,  $f_V$  is the velocity filling factor, and  $T_b$  is its rest frame brightness temperature, which can be estimated from the observed CO(9–8)/CO(4–3) ratio of 0.5 in CO luminosity. If both CO lines arise in the same volume, then our escape probability models yield intrinsic CO(4–3) and (9–8) brightness temperatures of 135 and 70 K respectively. For the observed CO luminosity and line width (Table 1), and  $f_V = 1$ , the formula indicates the lens magnifies the CO source 7 to 20 times. Hence the true radius of the CO source is 160 to 270 pc.

3) *If the dust continuum source size is 0."4 to 0."8, then the far-IR/sub-mm magnification is 7 to 30, and the true far-IR luminosity is (3 to 14)  $\times 10^{13} L_{\odot}$ .* Because of opacity effects, the far-IR source is likely to be smaller than the CO source, but larger than the optical source. Although we cannot measure a diameter for the dust source at the peak of the far-IR continuum, a reasonable guess is that it is about the same size as the CO source, or about twice the  $\sim 0".35$  extension derived from the H-band image by Ledoux et al. (1998). With a dust continuum source size of 0."4 to 0."8, and the apparent far-IR luminosity of  $1 \times 10^{15} L_{\odot}$  from the observations of Lewis et al. (1998), we use eq.(6) of Downes et al. (1995) to calculate the lens magnification of a 220 K blackbody, far-IR source to be

$$m_{\text{fir}} \equiv \frac{a_{\text{fir}}}{R_{\text{bb}}} = 4.17 \times 10^{-6} \frac{a_{\text{fir}}^2 (T_d/220 \text{ K})^4}{L_{\text{fir}}(\text{app})/(1 \times 10^{15})} \quad (3)$$

where  $a_{\text{fir}}$  is the apparent semi-major axis of the magnified far IR source, in pc,  $T_d$  is the dust temperature in K, and  $L_{\text{fir}}$  is the apparent far-IR luminosity in  $L_{\odot}$ . This then yields a far-IR/sub-mm magnification of 7 to 30, meaning that the true radius of the far-IR/sub-mm source is 90 to 180 pc, and the true far-IR luminosity is (3 to 14)  $\times 10^{13} L_{\odot}$ .

4) *If the dust absorbs half the power of the quasar, then the optical/UV magnification factor is 14 to 60.* In most of the “warm” ultraluminous galaxies, the obscuring dust ring or

disk absorbs about half of the available power from the central source, and the rest escapes out the poles of the torus or disk (see the analysis of Mrk 231 in Downes & Solomon 1998). This implies the true optical/UV power input is twice the far-IR luminosity, so the apparent optical/UV luminosity of  $4 \times 10^{15} L_{\odot}$  corresponds to an optical/UV magnification of 14 to 60 by the gravitational lens. This is comparable with the optical magnification deduced for IRAS F10214+4724 (e.g., Broadhurst & Lehar 1995; Eisenhardt et al. 1996).

5) *The dust mass is (1 to 7)  $\times 10^7 M_{\odot}$ .* Because the dust is optically thin at observed wavelengths  $> 1.4$  mm (emitted wavelengths  $> 290 \mu\text{m}$ ), we can use the observed continuum flux and the derived magnification factor  $m_{\text{fir}}$  to estimate the dust mass from

$$M_{\text{d}} = \frac{S(\nu_{\text{obs}}) D_{\text{A}}^2 (1+z)^3}{m_{\text{fir}} \kappa_{\text{d}}(\nu_{\text{e}}) B(\nu_{\text{e}}, T_{\text{d}})} \quad , \quad (4)$$

where  $S$  is the flux density,  $\nu_{\text{obs}}$  and  $\nu_{\text{e}}$  are the observed and emitted frequencies,  $D_{\text{A}}$  is the emission distance (angular size distance),  $B$  is the Planck function, and  $T_{\text{d}}$  is the dust temperature (see, e.g., Downes et al. 1992). We use the dust absorption coefficient  $\kappa_{\text{d}} = 0.4 (\nu_{\text{e}}/250 \text{ GHz})^2 \text{ cm}^2$  per gram of *dust* (e.g. Krügel & Siebenmorgen 1994). This yields a dust mass of  $(1 \text{ to } 7) \times 10^7 M_{\odot}$ . For further discussion of uncertainties in the dust mass, see Hughes et al. (1997).

6) *The gas mass is (1 to 6)  $\times 10^9 M_{\odot}$ .* The gas is more problematic because the high optical depths of the CO(4–3) and (9–8) lines ( $\tau = 20$  to 40 in our models) would be consistent with the magnification model derived above and the apparent CO luminosities for a range of gas masses. Our estimate is based on a mean  $\text{H}_2$  density of  $4000 \text{ cm}^{-3}$  from the excitation modeling, and a true radius of 160 to 270 pc for the CO source, which we assume to be a disk with thickness-to-radius ratio of 0.3. The gas mass we quote is for  $\text{H}_2$  plus helium. In the excitation modeling, we assumed typical interstellar abundances in our Galaxy. The gas mass could be lower if the metal abundances are super-solar, as in the near-nuclear regions of many quasars.

The derived values also depend on the assumed cosmology. For  $q_0 = 0.5$  and  $h = H_0/50$ , our estimates of true size, gas mass, and dynamical mass scale as  $h^{-1}$ ,  $h^{-2}$ , and  $h^{-1}$ , respectively. Note that at  $z = 3.9$ , quantities derived with  $H_0 = 50 \text{ km s}^{-1} \text{ Mpc}^{-1}$  and  $q_0 = 0.5$  are the same as those derived with  $H_0 = 75 \text{ km s}^{-1} \text{ Mpc}^{-1}$  and  $q_0 = 0.15$ . We summarize our results in Table 2, where we interpret the optical/UV continuum as the emission of an accretion disk, and the CO lines and far-IR continuum as the emission of a larger, circumnuclear disk. For most entries in the Table, we give a range of values corresponding to the uncertainties in the source size, which yield solutions with low magnification (first value) and high magnification (second value). The low magnification solutions make the gas mass equal to the dynamical mass, so the true magnification is more

likely to lie in the middle to high end of the range.

In summary, as with other gravitationally lensed sources detected in CO and the millimeter dust continuum, we have a good idea of the intrinsic CO and far IR surface brightness of APM 08279+5255 at  $z = 3.9$ . We can therefore estimate the CO and far IR/sub-mm magnifications. Our results (Table 2) suggest the far IR and CO sources are magnified 7 to 30 times and have true radii of 90 to 270 pc. The true far IR luminosity is  $(3 \text{ to } 14) \times 10^{13} L_{\odot}$ . Because the CO and far IR magnifications are lower than the optical/UV magnification, the true total luminosity is of the order of  $(0.7 \text{ to } 3) \times 10^{14} L_{\odot}$ , with about half of the quasar’s power being absorbed in the surrounding dust. From the CO line width, we think this far-IR emitting dust is in a rotating nuclear disk. In dust and molecular gas content, this disk resembles closely the circumnuclear disk in the IR ultraluminous Seyfert 1 galaxy Mrk 231, with the critical difference that APM 08279+5255 is 25 to 100 times stronger than Mrk 231 in total intrinsic luminosity.

We thank the referee for numerous helpful comments. T.W. thanks the STScI Visitor Exchange Program for their hospitality during this work, and the Swedish National Science Council for their support.

## REFERENCES

- Broadhurst, T., & Lehar, J. 1995, ApJ, 450, L41
- Downes, D., Radford, S.J.E., Greve, A., Thum, C., Solomon, P.M., & Wink, J.E. 1992, ApJ, 398, L25
- Downes, D., Solomon, P.M., & Radford, S.J.E. 1995, ApJ, 453, L65
- Downes, D., & Solomon, P.M. 1998, ApJ, 507, 615
- Eisenhardt, P.R., Armus, L., Hogg, D.W., Soifer, B.T., Neugebauer, G., & Werner, M. 1996, ApJ, 461, 72
- Harrison, E.R. 1981 *Cosmology*, Cambridge,UK: Cambridge Univ. Press., 239
- Hughes, D.H., Dunlop, J.S., & Rawlings, S. 1997, MNRAS, 289, 766
- Irwin M. J. 1998, private communication
- Irwin, M.J., Ibata, R.A., Lewis, G.F., & Totten, E. 1998, ApJ, 505, 529
- Kneib, J.P., Alloin, D., Mellier, Y., Guilloteau, S., Barvainis, R., & Antonucci, R. 1998, A&A, 329, 827
- Krügel, E., & Siebenmorgen, R. 1994, A&A, 288, 929
- Ledoux C., Théodore B., Petitjean P., Bremer, M.N., Lewis G.F., Ibata R.A., Irwin M.J., & Totten E.J. 1998, A&A, 339, L77
- Lewis, G.G., Chapman, S.C., Ibata, R.A., Irwin, M.J., & Totten, E.J. 1998, ApJ, 505, L1
- Maloney, P.R., Begelman, M.C. & Rees, M.J. 1994, ApJ, 432, 606
- Serjeant, S., Rawlings, S., Lacy, M., McMahan, R.G., Lawrence, A., Rowan-Robinson, M., & Mountain, M. 1998, MNRAS, 298, 321
- Solomon, P.M., Downes, D., & Radford, S.J.E. 1992, ApJ, 398, L29
- Storrie-Lombardi, L.J., McMahan, R.G., Irwin, M.J., Hazard, C. 1996, ApJ, 468, 121
- White, R.L., Becker, R.H., Helfand, D.J., & Gregg, M.D. 1997, ApJ, 475, 479

Table 1. OBSERVATIONS OF APM 08279+5255

Parameter	CO(4–3)	CO(9–8)	3.2 mm dust	1.4 mm dust
Emitted frequency (GHz)	461.0408	1036.912	463.1	1051.0
Observed frequency (GHz)	$93.872 \pm 0.005$	$211.145 \pm 0.007$	94.3	214.0
Redshift (LSR)	$3.9114 \pm 0.0003$	$3.9109 \pm 0.0002$	—	—
Line width ( $\text{km s}^{-1}$ )	$480 \pm 35$	480 (adopted)	—	—
Peak flux density, $S$ (mJy)	$7.4 \pm 1.0$	$17.9 \pm 1.4$	$1.2 \pm 0.3$	$17.0 \pm 0.5$
Integrated flux ( $\text{Jy km s}^{-1}$ )	$3.7 \pm 0.5$	$9.1 \pm 0.8$	—	—

The table gives the statistical errors. In addition, systematic uncertainties in the flux scales are  $\pm 5\%$  at 3.2 mm and  $\pm 15\%$  at 1.4 mm.

Table 2. PROPOSED COMPONENTS OF APM 08279+5255

	CO(4-3) line	Far IR continuum	optical/UV continuum
Component	nuclear disk	nuclear disk	accretion disk
Apparent luminosity	$9.5 \times 10^{10} L_\ell$	$1 \times 10^{15} L_\odot$	$4 \times 10^{15} L_\odot$
Apparent diam. (arcsec)	0.6 — 1.0	0.4 — 0.8	$(7 - 14) \times 10^{-5}$
Magnification	7 — 20	7 — 30	14 — 60
True luminosity	$(17 - 6) \times 10^9 L_\ell$	$(14 - 3) \times 10^{13} L_\odot$	$(29 - 7) \times 10^{13} L_\odot$
Temperature (K)	$T_{\text{kin}} = 200$	$T_{\text{dust}} = 220$	$T_{\text{acc.disk}} = 30000$
True radius (pc)	270 — 160	180 — 90	0.02 — 0.01
Gas mass (H <sub>2</sub> + He) (M <sub>⊙</sub> )	$(6 - 1) \times 10^9$	—	—
Dust mass (M <sub>⊙</sub> )	—	$(7 - 1) \times 10^7$	—
Dynamical mass (M <sub>⊙</sub> ) (if $V_{\text{rot}} = 300 \text{ km s}^{-1}$ )	$(6 - 3) \times 10^9$	—	—

Entries with a range of values correspond to low magnification (first value) and high magnification (second value). Masses are enclosed masses interior to the true radius. The CO line luminosity unit  $L_\ell$  is in  $\text{K km s}^{-1} \text{ pc}^2$ .

Adopted parameters for luminosities:  $H_0 = 50 \text{ km s}^{-1} \text{ Mpc}^{-1}$ ,  $\Omega = 1$ ,  $\Lambda = 0$ , emission distance (angular size distance) =  $D_A = 1.35 \text{ Gpc}$  ( $1'' = 6.54 \text{ kpc}$ ), reception distance (metric distance) =  $D_M = 6.63 \text{ Gpc}$ , age = 1.2 Gyr, lookback time = 11.9 Gyr, recession velocity at emission =  $2.5c$  (e.g. Harrison, 1981).

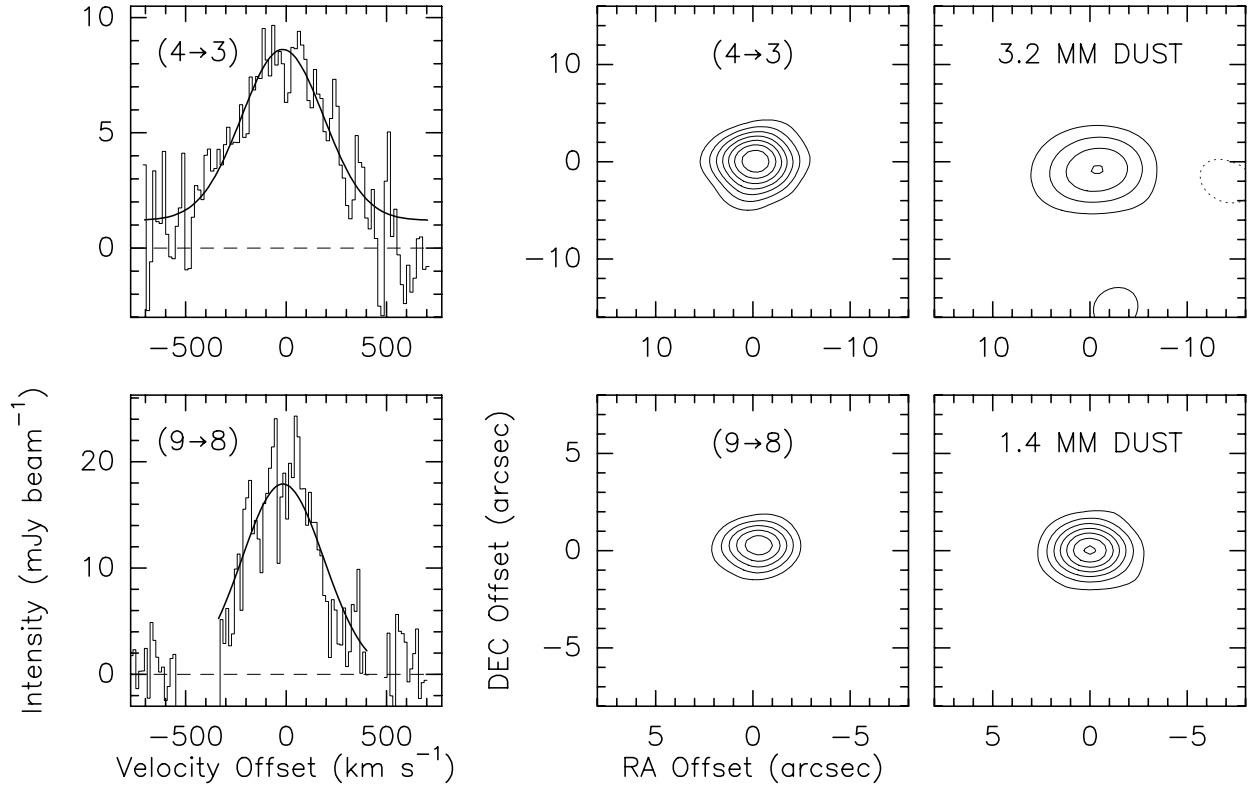


Fig. 1.— CO spectra and maps of APM 08279+5255. *Upper left:* CO(4-3) spectrum with resolution  $16 \text{ km s}^{-1}$ , velocities relative to  $93.867 \text{ GHz}$ ; the  $1.2 \text{ mJy}$  continuum was not subtracted. The central part of the line has more integration time and hence less noise than the line wings. *Lower left:* CO(9-8) spectrum with resolution  $14 \text{ km s}^{-1}$ , velocities relative to  $211.134 \text{ GHz}$ , and the  $17 \text{ mJy}$  continuum subtracted. The zero-level baseline insets right and left show the noise in the line-free sideband after continuum subtraction. Fitted Gaussians to both spectra have a width of  $480 \text{ km s}^{-1}$  (FWHM). *Upper center:* CO(4-3) intensity in a  $1000 \text{ km s}^{-1}$  wide band centered on  $93.867 \text{ GHz}$ , with the  $1.2 \text{ mJy}$  subtracted. Contour step =  $0.5 \text{ mJy beam}^{-1}$ . *Upper right:* The  $3.2 \text{ mm}$  dust continuum in a  $500 \text{ MHz}$  wide band centered on  $94.3 \text{ GHz}$ . Contour step =  $0.5 \text{ mJy beam}^{-1}$  ( $1.7 \sigma$ ). *Lower center:* CO(9-8) intensity in a  $760 \text{ km s}^{-1}$  wide band, with the  $17 \text{ mJy}$  continuum subtracted. Contour step =  $2 \text{ mJy beam}^{-1}$ . *Lower right:* The  $1.4 \text{ mm}$  dust emission in a  $450\text{-MHz}$  band centered on  $214.0 \text{ GHz}$ . Contour step =  $2 \text{ mJy beam}^{-1}$  ( $4\sigma$ ). Beams are  $6''.6 \times 5''.3$  (at  $3.2 \text{ mm}$ ) and  $3''.2 \times 2''.3$  (at  $1.4 \text{ mm}$ ). Offsets in all maps are relative to the CO and mm-dust source position,  $08^{\text{h}}31^{\text{m}}41^{\text{s}}.70$ ,  $52^{\circ}45'17''.35$  (J2000;  $\pm 0''.3$ ).